77 GHz High Gain Bull's-Eye Antenna With Sinusoidal Profile

U. Beaskoetxea, V. Pacheco-Peña, B. Orazbayev, T. Akalin, *Member, IEEE*, S. Maci, *Fellow, IEEE*, M. Navarro-Cía, *Member, IEEE*, and M. Beruete

***Abstract*— A high-gain Bull's-Eye leaky-wave horn antenna working at 77GHz with sinusoidal profile has been designed, fabricated and experimentally measured. The influence of the number of periods on the gain and beamwidth are numerically investigated. Experimental measurements show a high gain of 28.9dB, with low side-lobe level and a very narrow beam width in good agreement with results obtained from simulations.**

***Index Terms*—Leaky Wave Horn Antenna, Sinusoidal Profile, Bull's-Eye, Corrugated surface, Millimeter-waves**

I. Introduction

Leaky-wave antennas are a time honored research topic [1],[2]. In 1946, W. W. Hansen patented the first known leaky wave antenna, presented as a radiating electromagnetic waveguide capable of steering the radiating beam [3]. Two basic types of leaky wave antennas can be found: uniform [2],[4] and periodic antennas [2],[5].

Some years ago, periodic leaky wave antennas with very low profile and with broadside radiation were reported in the microwaves range [6]–[8] as an evolution of the work developed in [9]–[11]. The plasmonic explanation proposed in [9] was then complemented by a leaky-wave interpretation [12], [13]. Afterwards, similar antennas were proposed for quantum-cascade lasers [14].

Here, we present an evolution of the so-called Bull's-Eye antenna (i.e. central slot surrounded by annular corrugation), which was first presented in [15] and, soon after, in [6], by introducing a sinusoidal corrugation profile instead of the typical square corrugations or the recently investigated triangular corrugations [16]. A similar idea was also studied in [17], but there the surface was modulated by a sinusoidal spiral function, achieving a circularly polarized leaky wave antenna. In our antenna, a very high-gain as high as 28.9dB with a low side lobe level (-23.9dB) and very narrow beamwidth (1.2deg) is experimentally demonstrated at the W-band of the millimeter-waves, a frequency where automotive radar applications are proposed for on board navigation systems such as adaptive cruise control, object detection, blind spot detection, to name a few.

II. Prototype Design And Simulations

As shown in Fig. 1(a), the antenna consists of a metallic plate with a small central aperture surrounded by a sinusoidal periodic structure. The operation frequency selected is f = 77 GHz (λ = 3.89 mm).

The excitation of the antenna is done by using a standard waveguide (WR-10, W band) screwed to the back of the antenna. The power is coupled to the output by means of a slot resonance determined by the disc depth, t, and slot width, s_x, see Fig. 1(b).

In the final prototype, the minimum antenna thickness is constrained by the amplitude of the sinusoidal corrugation and the flange needed to attach the input waveguide to the antenna (UG-387/U MOD flange). The slot height, s_y, mainly governs the operation bandwidth and depth of resonance. In order to have a relatively high quality factor resonance, $s_y << \lambda$. The corrugated structure with period d and number of periods p starts at an optimized offset distance, o_1. At this offset distance currents are not affected by the reactive fields emerging from the radiating slot. It was also observed that including a small offset at the end of the disc, o_2, enhanced the side lobe level. This improvement can be ascribed to an

Manuscript received XX; revised XX; accepted XX. Date of publication XX; date of current version XX. This work was supported by the Spanish government under Grant Consolider Engineering Metamaterials CSD2008-0066 and Grant TEC2011-28664-C02-01. M. Navarro-Cía was supported by the Imperial College Junior Research Fellowship. M. Beruete was supported by the Spanish Government under the Research Contract Program Ramón y Cajal RYC-2011-08221 and by the European Science Foundation (ESF) for the activity entitled "New Frontiers in Millimetre/Sub-Millimetre Waves Integrated Dielectric Focusing Systems."

U. Beaskoetxea, V. Pacheco-Peña B. Orazbayev and M. Beruete are with the Antenna Group-TERALAB (MmW-THz-IR & Plasmonics Laboratory), Universidad Pública de Navarra, Pamplona 31006, Spain (e-mail: unai.beaskoetxea@unavarra.es,victor.pacheco@unavarra.es, b.orazbayev@unavarra.es, miguel.beruete@unavarra.es).

T. Akalin is with Institute of Electronics, Microelectronics and Nanotechnology (IEMN), Lille University, Lille, France (e-mail: Tahsin.Akalin@iemn.univ-lille1.fr).

S. Maci is with the Department of Information Engineering, University of Siena, Via Roma 56, 50124, Siena, Italy (e-mail: macis@dii.unisi.it).

M. Navarro-Cía is with the Optical and Semiconductor Devices Group, Department of Electrical and Electronic Engineering, Imperial College London, London SW7 2AZ, U.K., and also with the Centre for Plasmonics and Metamaterials and the Centre for Terahertz Science and Engineering, Imperial College London, London SW7 2AZ, U.K. (e-mail: m.navarro@imperial.ac.uk).

optimized termination for the travelling wave. As discussed in [6], [7], [14], broadside radiation takes place when the period of the corrugated structure is close to the wavelength, $d \approx \lambda$. With this condition, together with a proper grooves' dimensions tuning, the periodic structure radiates a narrow beam from the excitation of the n = -1 space harmonic (or Floquet mode).

The finite-integration time-domain software CST Microwave Studio™ was used to design and study the antenna where the metallization was modelled as a perfect electric conductor, since it is a good approximation for metals at millimeter-waves. Given the two-fold symmetry of the antenna, vertical electric and horizontal magnetic symmetries were applied to simulate only a quarter of it. The smallest hexahedral mesh cell was 0.08 × 0.08 × 0.05 mm to map accurately the geometry. To obtain the final design, an optimization routine, based on the Trust Region Framework algorithm was run, taking as a seed the theoretical parameters described above. The goal here was to obtain the highest possible directivity, along with the lowest side lobe level. The final dimensions for a p=20 period structure can be seen in Table I.

TABLE I

PARAMETERS FOR BULL'S-EYE SINUSOIDAL ANTENNA

Parameter	Value (mm)
Cosine Period, d	3.89
Cosine Amplitude, a	0.439
Offset1, o_1	5.117
Offset2, o_2	0. 883
Disc Thickness, t	3.439
Slot width, s_x	2.203
Slot height, s_y	0.6

The parameter S_{11} presents a resonance of about −16 dB at 77 GHz, Fig. 1(c). As shown in Fig. 2(a,b), for this frequency a clear enhancement is achieved in both E- and H-plane radiation patterns when the sinusoidal periodic structure is included. The directivity of the antenna with a sinusoidal perturbation is D = 29.38 dB (red curve) with an enhancement of about 24 dB compared to the slot (blue curve). A sharp lobe with a narrow −3 dB beamwidth θ_{-3dB} = 1.2 deg appears with a side lobe level below −21.4 dB taken at ±4.7 deg in the E-plane and θ_{-3dB} = 2.4 deg and −24.6 dB side lobe level in the H-plane.

As discussed in [12], for this type of leaky wave antennas consisting of a central slot surrounded by a periodic structure, pure broadside radiation (θ = 0 deg) is impossible due to the open stopband effect. In these antennas, radiation is conical and the parameters can be tuned to get the cone angle small enough to give a radiation in a nearly broadside single beam.

In other leaky-wave antenna designs [18], broadside radiation is achieved for microstrip structures with complex cells which include a quarter-wave transformer, or alternatively a matching stub.

In order to show more clearly the effect of including a periodic structure, the number of periods on the antenna was changed from 2 to 41 (i.e., the size of the antenna was changed) with the rest of parameters unchanged. Figure 3 presents the evolution of the directivity and beamwidth in the E-plane as a function of number of periods. The increase of the antenna size enables the leaky-wave to propagate longer, thus increasing the effective length and therefore, the directivity. Meanwhile, this improvement in the directivity is accompanied by a narrowing in the frequency bandwidth (inset in Fig.3). The larger the number of periods, the better the definition of the band (i.e., the higher the attenuation rate in filter jargon).

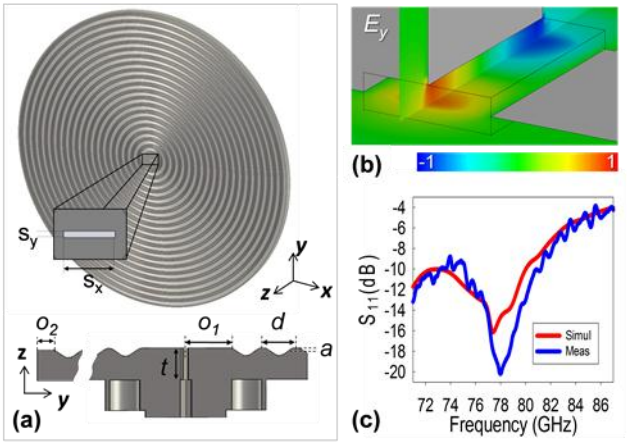

Fig. 1. Sinusoidal Bull's Eye antenna (a). Detail of the slot resonance (b). Measured (blue curve) and simulated (red curve) S_{11} (c).

A frequency scaled version of the Bull's-Eye antenna in [6] with square – instead of sinusoidal – corrugations was also studied for the same number of periods at 77 GHz, see Fig. 3. The directivity of the rectangular groove antenna (triangles in Fig. 3) overpasses that of the sinusoidal antenna for small number of periods (i.e., small radius), namely until the aperture efficiency relevant to the leaky-mode illumination is high enough [6]. When the aperture dimension reaches a certain limit value, the aperture tapering efficiency becomes too low and the directivity of the sinusoidally corrugated antenna (dots) becomes larger. Concerning the beamwidth (reported in the same Fig. 3), the two types of antennas exhibit a similar behaviour, presenting around θ_{-3dB} = 0.6 deg. From p=30 onwards, less than 1.3% (1 GHz) bandwidth was observed for both cases, whereas, regarding the aperture efficiency, values between 6% and 7% were obtained.

Due to the simulation workload for structures larger than p=41, only a single simulation was done for p=50, for which a 1dB higher gain was observed (38.3dB for the sinusoidal case).

III. EXPERIMENTAL MEASUREMENTS

A 20 period antenna was fabricated (by beamforming) as it was considered a good tradeoff between the

directivity and a reasonable dimension/cost. The raw material used for the structure manufacturing was ENAW-7075 (AlZn5.5MgCu). In the first step, called turning process, the disc with the sinusoidal surface is produced, followed by the milling process, where the flange geometry is drilled. Finally, a spark erosion process is applied whereby the rectangular waveguide (flange's and disc's slots) is eroded. The final result is shown in the inset in Fig. 4.

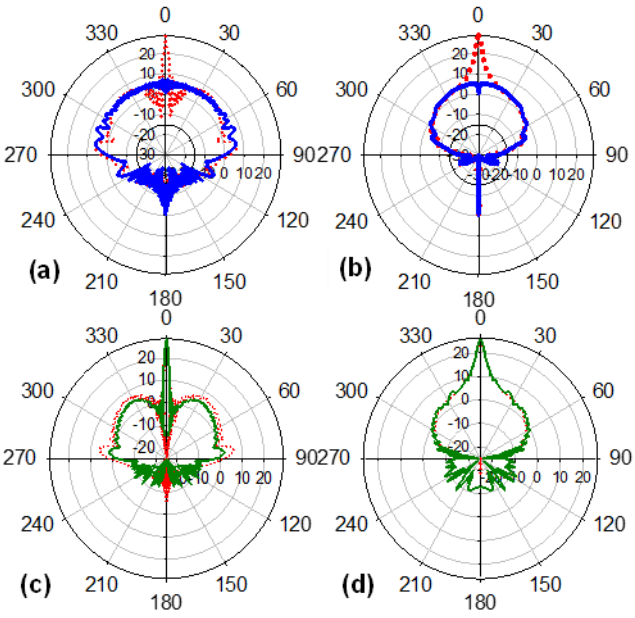

Fig. 2. Simulated radiation diagram comparisons for flat disc (blue curves) and sinusoidal Bull's Eye (red dotted curves): E-plane (a) and H-plane (b). Radiation diagram comparisons for simulated (red dotted curves) and measured (green curves) sinusoidal Bull's Eye: E-plane (c) and H-plane (d).

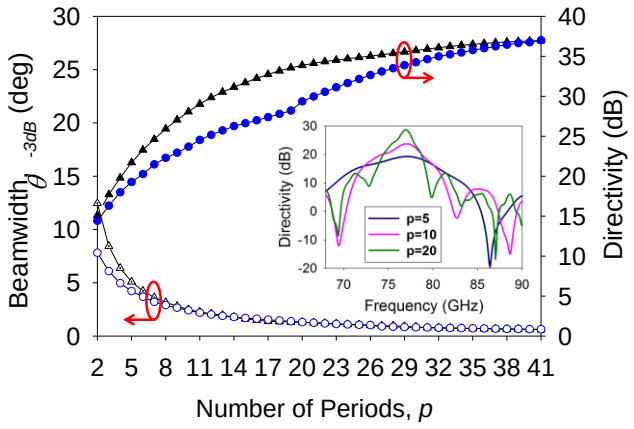

Fig. 3. Beamwidth (left hand scale) and Directivity (right hand scale) versus number of periods (one period is approximately equal to one wavelength) for square-grove corrugations (triangles) and sinusoidal corrugation (circles). (Inset) Directivity vs. frequency for 5, 10 and 20 period antennas.

For the experimental characterization of the antenna return loss and its radiation patterns, an ABmm Quasioptical Vector Network Analyzer together with a rotary platform (from 0 to 180 deg angle range) were employed. The test was done for the 71-87 GHz range.

To characterize the return loss, a calibration was done by placing a short-circuit (i.e. a mirror) at the output of the feeding waveguide, so that the reflection is maximum. Then the mirror was removed, and the antenna was connected. In order to avoid spurious effects due to reflections, the antenna was pointed towards an open area and, as a further caution, millimeter-wave absorbers were placed in the path. A good agreement is observed between simulated and measured S_{11} (Fig. 1(c)), with a slight frequency shift. Arguably, this might be due to mechanical tolerances.

To obtain the radiation diagram, two opposite platforms were placed with a separation of 3.10 m, far from the far-field condition (13 m) due to physical space and instrumentation restraints. On the first platform the software controllable rotary platform was placed, where both the reference horn antenna and the Bull's-Eye antenna were mounted. The antennas' center was located 1.10 m above the floor and 1.5 m below the ceiling. The receiver horn antenna was placed on the other platform and carefully aligned with the transmitter. The path between antennas, as well as the platforms, was covered with millimeter-wave absorbers to mimic anechoic chamber conditions. The calibration was done by measuring the free-space transmission placing two identical standard horn antennas face to face at the 3.10 m distance. To measure the polar radiation diagrams, the sinusoidal antenna was rotated from -10 to +10 deg, with a step of 0.1 deg, and from -180 deg to -10 deg and from 10 deg to 180 deg with a step of 1deg, from 71 to 87 GHz with a step of 50 MHz.

TABLE II

RADIATION CHARACTERISTICS FOR 20 PERIOD ANTENNA AT 77GHZ

Parameter	Simulation	Measurement
Directivity (dB)	29.38	28.9
θ_{-3dB} (deg)	1.2	1.2
Bandwidth (GHz)	2.8	3
Side Lobe Level (dB)	-21.4	-23.9

The sinusoidal Bull's-Eye antenna broadband gain was then obtained by applying the gain-transfer (gain comparison) or substitution method [19]. The curves shown in Fig. 4 compare the behavior of the simulated and fabricated prototypes. A gain peak of 28.9 dB around the working frequency is measured, approximately 7.9 dB higher than the reference horn antenna. Both simulated and measured Bull's-Eye antennas have a similar 4 GHz bandwidth with higher gain than the reference horn antenna. Some ripple within the operation bandwidth appears in the measurements, probably due to some undesired reflections in the experimental facilities.

As shown in Fig. 2(c,d), the polar radiation diagrams obtained from simulations and measurements at the design frequency match almost perfectly for both E- and H-planes. Table II summarizes the main parameters obtained from them.

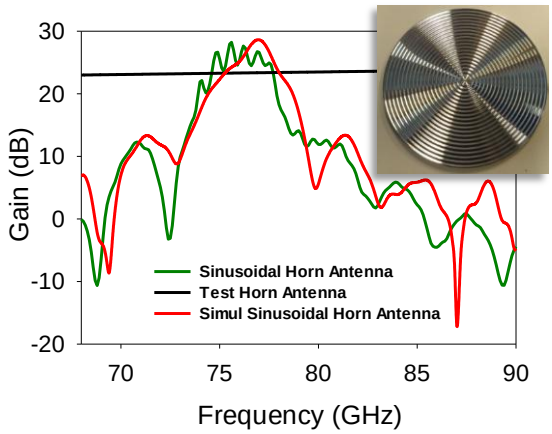

Fig. 4. Sinusoidal/Horn gain curves comparison. Inset: Manufactured Sinusoidal Bull's-Eye Antenna.

IV. Conclusions

A leaky-wave Bull's-Eye antenna with sinusoidal profile surface and working at 77 GHz has been designed, analyzed and measured. Several numerical studies have been performed to assess the performance of the antenna as a function of the number of periods with two different corrugation profiles, square and sinusoidal corrugations. In both cases, it is observed that the directivity (beamwidth) monotonically increases (decreases). The sinusoidal antenna has been experimentally characterized in the W-Band of the millimeter-wave spectrum.

A high gain of 28.9 dB, with side lobe level of -23.9 dB and 1.2º beamwidth, has been obtained in the measurements, in good agreement with the numerical simulations. It has been also demonstrated that sinusoidal and square corrugation profiles present very similar radiation characteristics. Nevertheless, the former can be of interest when medium/high power handling capabilities are required, since it does not present sharp corners that could lead to multipactor effects. These results could be of interest for novel antenna designs at millimeter waves and terahertz frequencies.

References

[1] A. A. Oliner, "Leaky-Wave Antennas," in *Antenna Engineering Handbook*, R. C. Johnson, Ed. New York: Mc Graw-Hill, 1993.

[2] L. O. Goldstone and A. A. Oliner, "Leaky-Wave Antennas I: Rectangular Waveguides," *IRE Trans. Antennas Propag.*, vol. 7, no. 4, 1959.

[3] W. W. Hansen, "Radiating Electromagnetic Wave Guide," 2402622, 1946.

[4] J. N. Hines, V. H. Rumsey, and C. H. Walter, "Travelling-Wave Slot Antennas," in *Proc. IRE*, 1950, vol. 40, pp. 1181–1188.

[5] M. Guglielmi and D. R. Jackson, "Broadside Radiation from Periodic Leaky- Wave Antennas," *IEEE Trans. Antennas Propag.*, vol. 41, no. 1, pp. 31–37, 1993.

[6] M. Beruete, I. Campillo, J. S. Dolado, E. Perea, F. Falcone, and M. Sorolla, "Very Low-Profile 'Bull' s-Eye' Feeder Antenna," *IEEE Antennas Wirel. Propag. Lett.*, vol. 4, no. 2, pp. 365–368, 2005.

[7] M. Beruete, I. Campillo, J. S. Dolado, E. Perea, F. Falcone, and M. Sorolla, "Dual-band low-profile corrugated feeder antenna," *IEEE Trans. Antennas Propag.*, vol. 54, no. 2, pp. 340–350, 2006.

[8] M. Beruete, I. Campillo, J. S. Dolado, E. Perea, F. Falcone, and M. Sorolla, "Low-Profile Corrugated Feeder Antenna," *IEEE Antennas Wirel. Propag. Lett.*, vol. 4, pp. 378–380, 2005.

[9] H. J. Lezec, A. Degiron, E. Devaux, R. A. Linke, L. Martin-Moreno, F. J. Garcia-Vidal, and T. W. Ebbesen, "Beaming light from a subwavelength aperture," *Science.*, vol. 297, no. 5582, pp. 820–822, 2002.

[10] M. Beruete, I. Campillo, J. S. Dolado, E. Perea, and M. Sorolla, "Enhanced Microwave Transmission and Beaming Using a Subwavelength Slot in Corrugated Plate," *IEEE Antennas Wirel. Propag. Lett.*, vol. 3, pp. 2002–2005, 2004.

[11] M. Beruete, M. Sorolla, I. Campillo, and J. S. Dolado, "Subwavelength slotted corrugated plate with enhanced quasioptical millimeter wave transmission," *IEEE Microw. Wirel. Components Lett.*, vol. 15, no. 4, pp. 286–288, Apr. 2005.

[12] D. R. Jackson, A. A. Oliner, T. Zhao, and J. T. Williams, "Beaming of light at broadside through a subwavelength hole: Leaky wave model and open stopband effect," *Radio Sci.*, vol. 40, no. 6, p. n/a–n/a, Dec. 2005.

[13] A. Sutinjo and M. Okoniewski, "A Simple Leaky-Wave Analysis of 1-D Grooved Metal Structure for Enhanced Microwave Radiation," *IEEE Trans. Antennas Propag.*, vol. 60, no. 6, pp. 2719–2726, 2012.

[14] N. Yu, J. Fan, Q. J. Wang, C. Pflügl, L. Diehl, T. Edamura, M. Yamanishi, H. Kan, and F. Capasso, "Small-divergence semiconductor lasers by plasmonic collimation," *Nat. Photonics*, vol. 2, no. 9, pp. 564–570, Jul. 2008.

[15] P. Baccarelli, P. Burghignoli, G. Lovat, and S. Paulotto, "A novel printed leaky-wave 'bull-eye' antenna with suppressed surface-wave excitation," in *IEEE Antennas and Propagation Society Symposium, 2004.*, 2004, vol. 1, pp. 1078–1081 Vol.1.

[16] M. Beruete, U. Beaskoetxea, M. Zehar, A. Agrawal, S. Liu, K. Blary, A. Chahadih, X. L. Han, M. Navarro-Cia, D. Etayo Salinas, A. Nahata, T. Akalin, M. Sorolla Ayza, M. Navarro-Cía, D. E. Salinas, and M. S. Ayza, "Terahertz Corrugated and Bull ' s-Eye Antennas," *IEEE Trans. Terahertz Sci. Technol.*, vol. 3, no. 6, pp. 740–747, 2013.

[17] G. Minatti, F. Caminita, M. Casaletti, and S. Maci, "Spiral Leaky-Wave Antennas Based on Modulated Surface Impedance," *IEEE Trans. Antennas Propag.*, vol. 59, no. 12, pp. 4436–4444, Dec. 2011.

[18] S. Paulotto, P. Baccarelli, F. Frezza, and D. R. Jackson, "Full-wave modal dispersion analysis and broadside optimization for a class of microstrip CRLH leaky-wave antennas," *IEEE Trans. Microw. Theory Tech.*, vol. 56, no. 12, pp. 2826–2837, 2008.

[19] IEEE, "IEEE Standard Test Procedures for Antennas," pp. 1–129, 1979.